

## Research Article

# Decomposition and Oriented Growth of $\text{YBa}_2\text{Cu}_3\text{O}_{7-x}$ Films Prepared with Low Fluorine TFA-MOD Approach

Xiaohui Zhao, Pan Zhang, Yabing Wang, Jie Xiong, and Bowan Tao

State Key Laboratory of Electronic Thin Film and Integrated Devices, University of Electronic Science and Technology of China, Chengdu 610054, China

Correspondence should be addressed to Xiaohui Zhao; xhzhao@uestc.edu.cn

Received 26 September 2013; Accepted 28 October 2013

Academic Editor: Jianhua Hao

Copyright © 2013 Xiaohui Zhao et al. This is an open access article distributed under the Creative Commons Attribution License, which permits unrestricted use, distribution, and reproduction in any medium, provided the original work is properly cited.

TFA-MOD approach of  $\text{YBa}_2\text{Cu}_3\text{O}_{7-x}$  (YBCO) films has been approved to be the most promising method for mass production of low cost high temperature coated conductors. In order to reduce the decomposition time and improve the properties of YBCO films, copper propionate was used as the precursor and certain Lewis-bases were introduced into the precursor solution. The fluorine content of the solution was significantly reduced. High quality oriented YBCO films were prepared on LAO substrates with this low fluorine TFA-MOD approach. The effects of the sintering temperature on the oriented growth and properties of YBCO films were investigated. The preliminary results yielded the critical current density ( $J_c$ ) of  $2 \text{ MA/cm}^2$  and critical current ( $I_c$ ) of  $120 \text{ A/cm}$  width at  $77 \text{ K}$  and self-field.

## 1. Introduction

Second generation  $\text{YBa}_2\text{Cu}_3\text{O}_{7-x}$  (YBCO) high temperature superconducting materials have been considered as the most promising candidate for electric power applications due to their large critical current density ( $J_c$ ) at liquid nitrogen temperature ( $77.3 \text{ K}$ ) and high irreversibility field. Among all kinds of fabrication methods, the metal organic deposition (MOD) [1, 2] could provide precise composition control and large area deposition accessibility with low cost, which makes it appealing for large scale production. The conventional MOD route used trifluoroacetate salts as the precursors. However, due to high fluorine content in the precursor, large amount of HF gas is generated during the decomposition. In order to avoid crack of the film, the heating rate during decomposition is generally kept below  $1^\circ\text{C}/\text{min}$ . This results in long term decomposition process over 20 hours. Seeking for reducing the decomposition time without degradation of the film quality, a different precursor has been introduced to substitute trifluoroacetate salts or modify the chemistry of the precursor solution [3–10]. Fuji et al. [3] and Tokunaga et al. [4] chose copper naphthenate as the copper precursor, the decomposition time was reduced, and high performance

YBCO film with  $I_c$  over  $200 \text{ A/cm}$  width was achieved. However, as a complex mixture distilled from petroleum, copper naphthenate comprises of certain petroleum by-products and contaminants. So the composition of copper naphthenate is not stable and the copper content varies, which makes the precise control of the film composition and fabrication of long tape with uniform performance almost impossible.

In this report, copper propionate was used to substitute copper trifluoroacetate, and with this substitution the fluorine content of the precursor was reduced around 50%. The decomposition process of the precursor film was adjusted accordingly. The effects of the sintering temperature on the microstructure and oriented growth of the YBCO film were discussed in detail.

## 2. Experimental

Y, Ba, and Cu acetate salts are used as the starting materials for the precursor solution preparation. Yttrium acetate and barium acetate were dissolved in water with Y/Ba ratio of 1:2 and reacted with excessive trifluoroacetate acid at  $80^\circ\text{C}$  for 6 hours. The resulting solution was refined under reduced

pressure to remove water and excessive acid. Meanwhile, Cu acetate was dissolved in methanol and reacted with excess propionate acid at 80°C for 2 hours. And appropriate amount of diethanolamine (DEA) and ammonia was added dropwise into the solution. Two solutions prepared above were mixed together with Y:Ba:Cu ratio of 1:2:3 at room temperature and concentrated under vacuum, resulting in a viscous and deep blue precursor solution. Only removal of volatile solvents was conducted during the whole process; therefore the content of metal ions in final precursor solution is consistent with the starting materials, which offers the feasibility of precise composition control. Methanol was used as the solvent and the total metal ion concentration of the solution was adjusted to 2 mol/L.

The precursor solution was spin-coated onto the (001) oriented LaAlO<sub>3</sub> single crystal substrate with spinning rate of 3000 rpm for 60 seconds. The precursor film was baked at hot plate for 60 seconds afterwards and decomposed in the tube furnace with 1.3% humidified oxygen. The heating profile was shown in Figure 2. The whole decomposition process takes less than 2 hours; comparing with more than 20 hours for conventional TFA-MOD, this is a significant improvement in efficiency and potentially reducing manufacturing cost. Homogeneous and crack-free film consisting intermediate phase, for example, Y<sub>2</sub>O<sub>3</sub>, BaF<sub>2</sub>, and CuO, was achieved [11, 12]. And then the decomposed film was crystallized at 790–830°C for 1 hour under humid oxygen and argon balanced atmosphere. Afterwards the films were annealed at 500°C with dry oxygen to form superconducting phase.

Differential thermal analysis (DTA) and thermal gravimetric analysis (TGA) of precursor solution were performed in air with a 2°C/min heating rate. The phase purity and microstructure of YBCO film were characterized with X-ray diffraction  $\theta$ -2 $\theta$  scans (HRXRD, Bede D1). The in-plane texture of YBCO film was quantified by measuring full width half maxima (FWHM) of YBCO (103)  $\Phi$ -scans. The rocking curve of the YBCO (005) peaks was measured to characterize the out-of-plane texture (*c*-axis alignment) of the film. The oriented growth mode of the film was revealed by XRD Chi-scan of YBCO (102) peaks. Surface morphology of films was examined by scanning electron microscopy (SEM). Film thickness was measured by DEKTA surface profiler. Critical current density ( $J_c$ ) of the film was determined by the  $J_c$ -scan Leipzig system.  $I_c$  was calculated from the  $J_c$  results and the thickness measured from the surface profiler.

### 3. Results and Discussion

In our precursor solution, copper propionate was used to substitute copper trifluoroacetate and the fluorine content of the precursor was reduced around 50%. So less HF gas will be generated with current approach.

**3.1. Decomposition of the Precursor.** In order to better understand the decomposition behavior of the precursor and redesign the heating profile of the decomposition process, DTA and TGA analyses were performed for gels dried from the precursor solution. As shown in Figure 1, there are two exothermic peaks in DTA curve located at 206°C and 240°C,

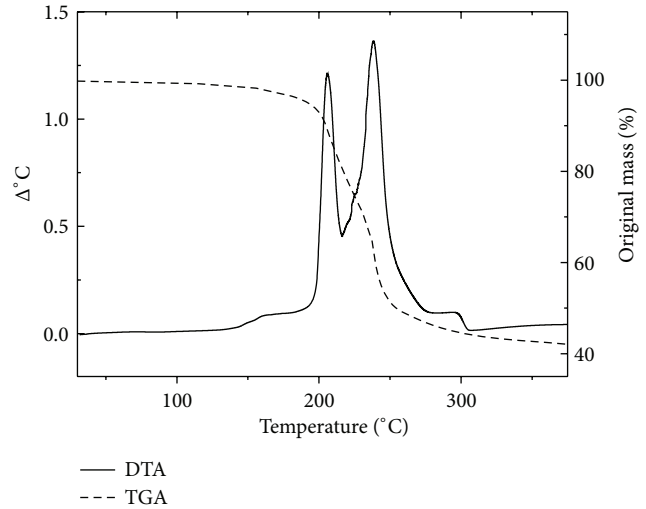
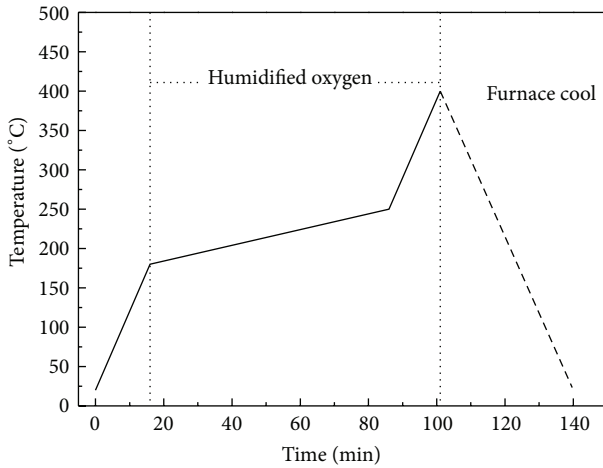


FIGURE 1: DTA and TGA curves for low fluorine TFA-MOD precursor gel decomposed in air.

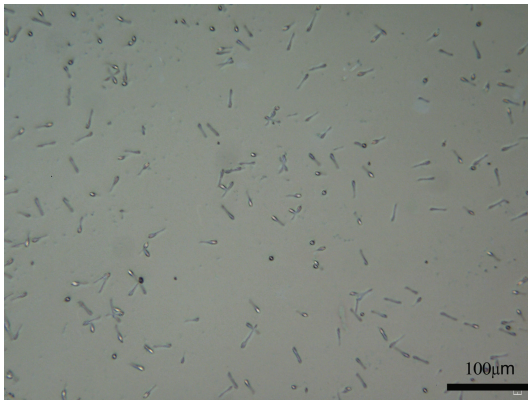
respectively. Compared with the traditional TFA-MOD precursor, which has only one intense exothermic peak at 260°C [13], the decomposition behavior becomes moderate. The first peak corresponds to Cu propionate decomposition, and the second exothermic peak at 240°C, which is believed to be resulting from the decomposition of Y- and Ba-trifluoroacetate. Surprisingly, both of these exothermic peaks shift to lower temperature in comparison with the expected value [13]. Significant weight loss between two exothermic peaks was observed and no substantial weight loss at higher temperatures, indicating that the decomposition of all the organic species was completed by 240°C. This phenomenon suggests that the introduction of DEA and Lewis-basic ammonia has dramatically affected the chemistry of the precursor solution.

Right after the volatile solvent evaporation at the beginning of the decomposition, the metal ions in the precursor film tend to cross-link with each other and aggregate to form clusters, especially for Cu, which have bigger ionic size. It is believed that the presence of Lewis-base can coordinate with metal ions, thereby reducing cross-linking of them during intermediate formation. Both DEA and ammonia has the Lewis-basic nature; after coordinating with metal ions, the cross-linking and aggregation of metal ions are significantly reduced. This is the key factor to account for that the decomposition becomes moderate and shifts to lower temperatures. In addition, less aggregation also reduces the segregation of the intermediate phase, and this ensures the chemical homogeneity and integrity of the film. On the other hand, the molecular weight of compound is increased by this coordination; as a consequence, the sublimation of Cu is suppressed, leading to reproducible stoichiometry of Y:Ba:Cu = 1:2:3.

The introduction of highly viscous DEA induced the viscosity increase of the precursor solution; however, the high boiling point of DEA (268°C) also makes it persistent in the film up to high temperature, leading to thermal



(a)



(b)

FIGURE 2: Heating profile of decomposition (a) and morphology (obtained with optical microscope) (b) of the precursor film.

stress relaxation of the precursor film. This explains that the smooth and crack free film still can be achieved even with faster heating rate. Both of these effects enable the rapid decomposition of precursor films with increased thickness.

Based on TGA and DTA results, the heating profile of decomposition was modified accordingly. The ramp rate of  $1^{\circ}\text{C}/\text{min}$  was applied for the temperature range  $200^{\circ}\text{C}$ – $250^{\circ}\text{C}$  in which major decomposition happened and fast ramp rate of  $10^{\circ}\text{C}/\text{min}$  was used beyond this range. As shown in Figure 2(a), the modified decomposition process could be complete in two hours, which is much less than that of the conventional TFA-MOD method. And the decomposed film is smooth and crack free with only uniform submicron pores resulting from the generation of HF gas, as shown in Figure 2(b). The thickness of the final YBCO film was determined to be 600 nm, which was almost doubled in comparison with that of traditional TFA-MOD method.

**3.2. Heating Rate Effect during Sintering.** The resulting decomposed film was further heated to higher temperature to form YBCO superconducting phase. The temperature window for superconducting phase is relatively small and

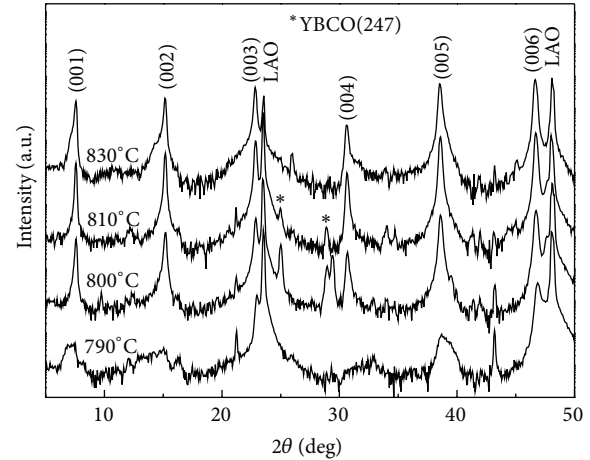


FIGURE 3: XRD  $\theta$ - $2\theta$  patterns of YBCO films with different sintering temperature. YBCO247 phase is marked with “\*”.

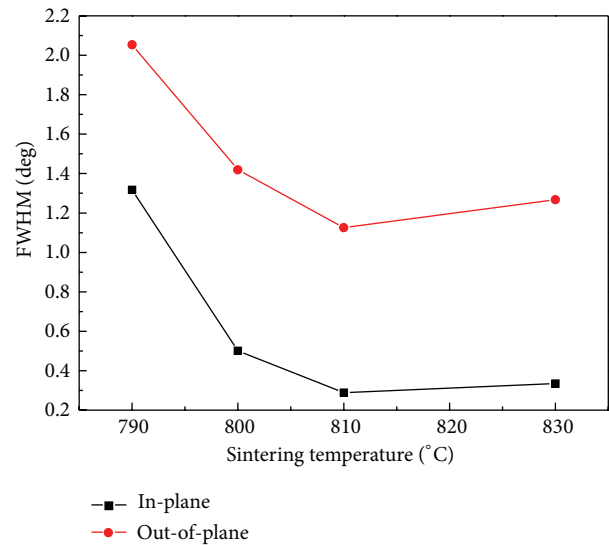


FIGURE 4: Temperature dependence of FWHM of in-plane and out-of-plane scan of YBCO films.

the sintering temperature is critical for the oriented growth of YBCO films. Different sintering temperatures ranging from 790 to  $830^{\circ}\text{C}$  were attempted while keeping other working conditions constant. XRD  $\theta$ - $2\theta$  scan of all the films was shown in Figure 3. The ordinate was put in log scale for details. All of the samples showed well-developed (001) growth with only slight amount of  $\text{Y}_2\text{Ba}_4\text{Cu}_7\text{O}_{15-x}$  phase at certain temperature. The temperature dependence of FWHM of rocking curve and out-of-plane scan was shown in Figure 4. Both of them reduced substantially with increasing temperature. At  $810^{\circ}\text{C}$ , the FWHM values of in-plane and out-of-plane scan were  $1.12^{\circ}$  and  $0.29^{\circ}$ , indicating high quality oriented growth of YBCO films.

In order to further disclose the temperature effect on the oriented growth of YBCO films, XRD Chi-scan of YBCO (102) was also performed. As shown in Figure 5, the peak

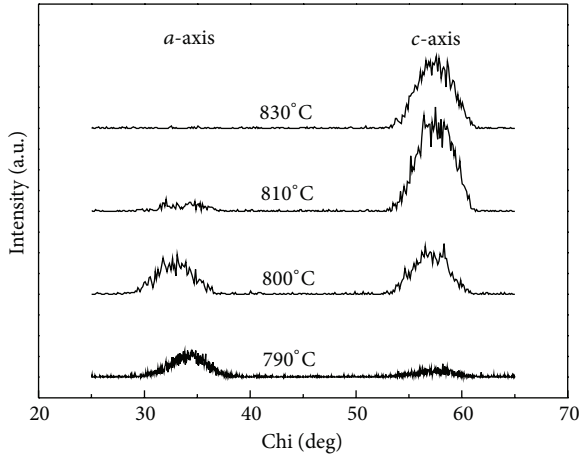


FIGURE 5: XRD Chi-scan of YBCO films with different sintering temperatures.

at  $35^\circ$  represents *a*-axis growth of YBCO. The intensity of the peak is dominant at  $790^\circ\text{C}$ , whereas the peak at  $57^\circ$  indicating *c*-axis growth is weak at low temperature. However, the peak intensity at  $57^\circ$  was significantly enhanced with increasing temperature while the peak at  $35^\circ$  was gradually diminished. This peak intensity variation indicates that with increasing sintering temperature, the oriented growth mode changed from *a*-axis growth to *c*-axis growth. And pure *c*-axis growth was achieved at  $830^\circ\text{C}$ . This result is coincident with previous studies and the similar growth thermodynamic properties have also been observed in perovskite oxides such as  $\text{SrTiO}_3$  and  $\text{BaTiO}_3$  [14–16]. It is widely accepted that the oriented growth of YBCO starts from the interface between intermediate phase and LAO substrate [17]. The lattice mismatch of *a*-axis and *c*-axis growth with LAO substrate is 0.8% and 1.9%, respectively. And thereby *c*-axis growth of YBCO requires larger thermodynamic driving force than *a*-axis growth, leading to preferred *a*-axis growth at relatively low temperatures.

**3.3. Properties of YBCO Films.** YBCO films were sintered at different temperatures for 1 hour alongside with other tailored working conditions. Figure 6 shows the morphology of YBCO film sintered at  $810^\circ\text{C}$ . Despite the existence of few needle-like *a*-axis grains, most part of the film shows well-connected, pallet-like *c*-axis grains. This SEM observation is consistent with the XRD results above. The superconductivity of all the films was measured and the variation of critical current density ( $J_c$ ) as a function of sintering temperature was shown in Figure 7. It is evident that  $J_c$  of YBCO films increased with sintering temperature, which can be ascribed to the increase of the *c*-axis growth. High  $J_c$  of  $2\text{ MA/cm}^2$  and  $I_c$  of  $120\text{ A/cm}$  width at  $77\text{ K}$  and self-field were obtained for YBCO film sintered at  $810^\circ\text{C}$ . However, only  $1\text{ MA/cm}^2$  was achieved at  $830^\circ\text{C}$ , which shows pure *c*-axis growth. This property degradation may be caused by other deteriorated features (such as interconnection) of YBCO grains after high temperature sintering. The relevant study is in progress.

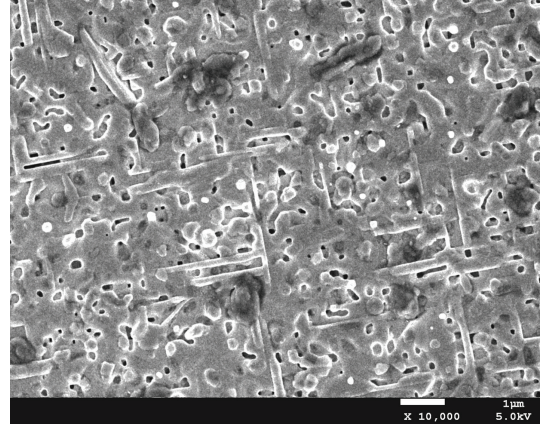


FIGURE 6: SEM (secondary electron) micrographs of the typical morphology of YBCO films sintered at  $810^\circ\text{C}$ .

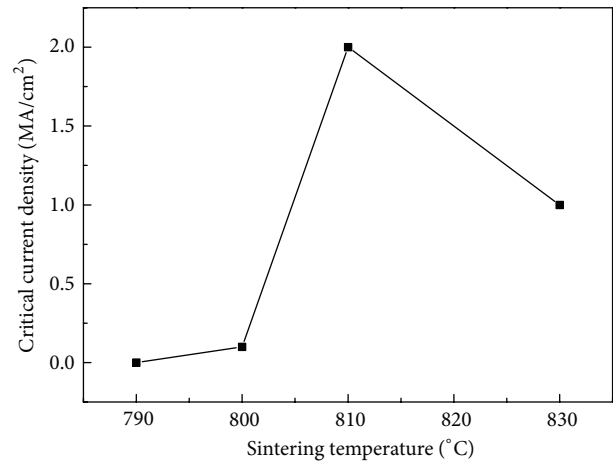


FIGURE 7: Critical current density ( $J_c$ ) of YBCO films as a function of sintering temperature.

## 4. Conclusion

High quality single-coating YBCO films with  $600\text{ nm}$  in thickness was prepared with low fluorine TFA-MOD approach. The decomposition process was shortened in 2 hours by Cu-propionate substitution and the introduction of Lewis-basic DEA and ammonia. Since the thermodynamic driving force for *c*-axis growth of YBCO is larger than that of *a*-axis growth, YBCO films undergo *a*-axis growth at low sintering temperature, whereas pure *c*-axis oriented growth is achieved at  $830^\circ\text{C}$ . High quality YBCO film with  $J_c$  of  $2\text{ MA/cm}^2$  and  $I_c$  of  $120\text{ A/cm}$  width at  $77\text{ K}$  and self-field was obtained.

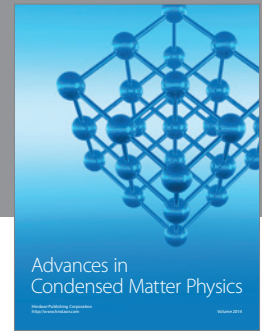
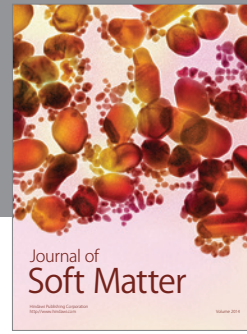
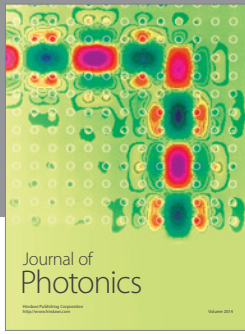
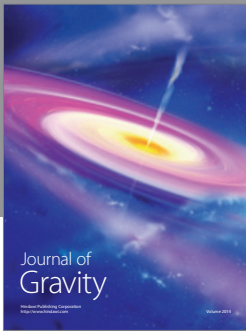
## Acknowledgments

This work was financially supported by National Natural Science Foundation of China (51002024), the Scientific Research Foundation of the State Human Resource Ministry, the Education Ministry for Returned Chinese Scholars, and the Fundamental Research Funds for the Central Universities. This work was also supported by a Grant to Dr. Wen Huang

from the National Natural Science Foundation of China (51002022).

## References

- [1] A. Gupta, R. Jagannathan, E. I. Cooper, E. A. Giess, J. I. Landman, and B. W. Hussey, "Superconducting oxide films with high transition temperature prepared from metal trifluoroacetate precursors," *Applied Physics Letters*, vol. 52, no. 24, pp. 2077–2079, 1988.
- [2] P. C. McIntyre, M. J. Cima, J. J. A. Smith, R. B. Hallock, M. P. Siegal, and J. M. Phillips, "Effect of growth conditions on the properties and morphology of chemically derived epitaxial thin films of  $\text{Ba}_2\text{Cu}_3\text{O}_{7-x}$  on (001)  $\text{LaAlO}_3$ ," *Journal of Applied Physics*, vol. 71, no. 4, pp. 1868–1877, 1992.
- [3] H. Fuji, T. Honjo, R. Teranishi et al., "Processing for long YBCO coated conductors by advanced TFA-MOD process," *Physica C*, vol. 412–414, pp. 916–919, 2004.
- [4] Y. Tokunaga, H. Fuji, R. Teranishi et al., "High critical current YBCO films using advanced TFA-MOD process," *Physica C*, vol. 412–414, pp. 910–915, 2004.
- [5] Y. Xu, A. Goyal, K. Leonard, and P. Martin, "High performance YBCO films by the hybrid of non-fluorine yttrium and copper salts with Ba-TFA," *Physica C*, vol. 421, no. 1–4, pp. 67–72, 2005.
- [6] Y. R. Patta, D. E. Wesolowski, and M. J. Cima, "Aqueous polymer-nitrate solution deposition of YBCO films," *Physica C*, vol. 469, no. 4, pp. 129–134, 2009.
- [7] D. Shi, L. Wang, J. Kim et al., "YBCO film with Sm addition using low-fluorine TFA-MOD approach," *IEEE Transactions on Applied Superconductivity*, vol. 19, no. 3, pp. 3208–3211, 2009.
- [8] X. H. Zhao, C. Gao, Y. D. Xia et al., "Preparation of YBCO coated conductors on RABiTS substrate with advanced TFA-MOD method," *Rare Metal Materials and Engineering*, vol. 40, pp. 342–345, 2011.
- [9] Y. Xu, Z. Qian, Z. Xu, P. He, M. Massey, and R. Bhattacharya, "Nucleation study of  $\text{YBa}_2\text{Cu}_3\text{O}_{7-x}$  (YBCO) films by modified tfa-mod approach," *IEEE Transactions on Applied Superconductivity*, vol. 19, no. 3, pp. 3127–3130, 2009.
- [10] X. Obradors, T. Puig, S. Ricart et al., "Growth, nanostructure and vortex pinning in superconducting  $\text{YBa}_2\text{Cu}_3\text{O}_{7-x}$  thin films based on trifluoroacetate solutions," *Superconductor Science and Technology*, vol. 25, no. 12, Article ID 123001, 2012.
- [11] R. Feenstra, F. A. List, X. Li et al., "A modular ex situ conversion process for thick MOD-fluoride RBCO precursors," *IEEE Transactions on Applied Superconductivity*, vol. 19, no. 3, pp. 3131–3135, 2009.
- [12] K. Zalamova, A. Pomar, A. Palau, T. Puig, and X. Obradors, "Intermediate phase evolution in YBCO thin films grown by the TFA process," *Superconductor Science and Technology*, vol. 23, no. 1, Article ID 014012, 2010.
- [13] J. T. Dawley, P. G. Clem, T. J. Boyle, L. M. Ottley, D. L. Overmyer, and M. P. Siegal, "Rapid processing method for solution deposited  $\text{YBa}_2\text{Cu}_3\text{O}_{7-x}$  thin films," *Physica C*, vol. 402, no. 1–2, pp. 143–151, 2004.
- [14] W. Huang, Z. P. Wu, and J. H. Hao, "Electrical properties of ferroelectric  $\text{BaTiO}_3$  thin film on  $\text{SrTiO}_3$  buffered GaAs by laser molecular beam epitaxy," *Applied Physics Letters*, vol. 94, no. 3, Article ID 032905, 2009.
- [15] W. Huang, J. Y. Dai, and J. H. Hao, "Structural and resistance switching properties of  $\text{ZnO}/\text{SrTiO}_3/\text{GaAs}$  heterostructure grown by laser molecular beam epitaxy," *Applied Physics Letters*, vol. 97, no. 16, Article ID 162905, 2010.
- [16] J. S. Wu, C. L. Jia, K. Urban, J. H. Hao, and X. X. Xi, "Microstructure and misfit relaxation in  $\text{SrTiO}_3/\text{SrRuO}_3$  bilayer films on  $\text{LaAlO}_3(100)$  substrates," *Journal of Materials Research*, vol. 16, no. 12, pp. 3443–3450, 2001.
- [17] T. G. Holesinger, L. Civale, B. Maiorov et al., "Progress in nano-engineered microstructures for tunable high-current, high-temperature superconducting wires," *Advanced Materials*, vol. 20, no. 3, pp. 391–407, 2008.



**Hindawi**

Submit your manuscripts at  
<http://www.hindawi.com>

